■ 18

A Numerical Modeling for Study Marine Current in the Manado Bay, North Sulawesi

Parabelem Tinno Dolf Rompas*, Jenly Dyliep Isria Manongko
Universitas Negeri Manado, Tondano, Indonesia
Jl. Kampus FT-Unima Tondano 95618, North Sulawesi, Indonesia, +62431322543
*Corresponding author, e-mail: parabelemrompas@unima.ac.id

Abstract

This study is investigating about marine currents provided electrical energy through the numerical model. The objective of this study is to know the power available distributions in the Manado Bay, North Sulawesi, Indonesia. The Manado Bay was width 2200 m with 79 m of depth. In computation, we are made grids in x and y horizontal were 7 m respectively, also for z vertical of four layers. The results shown that the power available distributions in the Manado Bay at 0.1 Sv were 0.00-20.00 kW/m² when low tide currents and when high tide currents were 0.00-105 kW/m². The values will enable for marine currents power plant in the Manado Bay to future.

Keywords: numerical model, marine currents, the Manado Bay, power available

1. Introduction

Numerical methods are one completion to determine the power available in Manado Bay. Already many researchers are investigating on numerical methods for ocean currents such as Casulli and Cheng in [1] that study on numerical method in San Francisco Bay, California and Lagoon of Venice, Italy. They simulated flooding and drying of tidal mud-flats in conjunction by 3D flows. Clement, et al., in [2] that developed numerical models in Bering Sea in North Pacific which have investigated the short-term marine circulation and flux in a small geographic region. Zarrati and Jin in [3] developed the mathematical model for 3D simulation into multi-layer model. Their models were able to predict diverse three-dimensional flow conditions through the velocity distribution and secondary flows. Rompas and Manongko [4] have studied on velocities of marine current in Bunaken Strait, North Sulawesi, Indonesia by numerical simulation. Draper, et al., [5] simulated energy potential of a tidal near a coastal headland using 2D depth averaged numerical model. Numerical experiments of tidal currents near New River inlet, NC, USA are conducted by Chen, et al., [6]. The Reynolds-averaged Navier-Stokes (RANS) equations as the basic equations used to solve numerical modeling [7-9]. The numerical models of tidal currents are developed such as in a coastal ocean (Maine Gulf, Fundy Bay, Minas Passage, and Minas Basin in North America) with subgrid approximation [10], in the Gold Coast Seaway area, Gold Coast, Australia [11] with simulations of flow, wave, and sediment transport. The evolution of tidal creek has studied by Gu, et al., [12]. Elzalabani, et al., [13] have presented the mathematical modeling and simulation tidal current energy that can be modeled as a stream of harmonics and applicated in building the tidal barrage across a bay.

In this study, we have used a numerical model that developed from [1-3]. Also, we want to investigate the power available distributions in the Manado Bay, North Sulawesi, Indonesia which influenced by Singkil river, refer to Figure 3.

2. Theory
2.1. Mathematical Model

The governing equations used to get the distributions of the power available from basic RANS Equations [14]. The model of Equations become:

$$\frac{\partial \bar{u}}{\partial t} + \bar{u}\frac{\partial \bar{u}}{\partial x} + \bar{v}\frac{\partial \bar{u}}{\partial y} + \bar{w}\frac{\partial \bar{u}}{\partial z} = -g\frac{\partial \eta}{\partial x} + div\left(v_{eff}\overrightarrow{grad}(\bar{u})\right) + f_{cor}\bar{v} \tag{1}$$

$$\frac{\partial \bar{v}}{\partial t} + \bar{u}\frac{\partial \bar{v}}{\partial x} + \bar{v}\frac{\partial \bar{v}}{\partial y} + \bar{w}\frac{\partial \bar{v}}{\partial z} = -g\frac{\partial \eta}{\partial y} + div\left(v_{eff}\overrightarrow{grad}(\bar{v})\right) - f_{cor}\bar{u} \tag{2}$$

$$\frac{\partial \bar{u}}{\partial x} + \frac{\partial \bar{v}}{\partial y} + \frac{\partial \bar{w}}{\partial z} = 0 \tag{3}$$

where $\bar{u}$ (x,y,z,t), $\bar{v}$ (x,y,z,t), and $\bar{w}$ (x,y,,z,t) are the velocities in horizontal directions of x, y, and z-direction respectively, $\eta(x,y,t)$ is the elevation of free surface, t is the time, v_{eff} is an effective diffusion taking of account turbulent viscosity and dispersion, $v_{eff} = v + v_t$, f_{cor} is the Coriolis parameter, assumed to be constant, and g is the gravity.

2.1.1. Turbulence Model
The equation of turbulence that used was turbulent viscosity from the mixing-length model [15, 16] as follow:

$$v_t = \left(l_h^4\left[2\left(\frac{\partial \bar{u}}{\partial x}\right)^2 + 2\left(\frac{\partial \bar{v}}{\partial y}\right)^2 + \left(\frac{\partial \bar{v}}{\partial x} + \frac{\partial \bar{u}}{\partial y}\right)^2 \right] + l_v^4\left[\left(\frac{\partial \bar{u}}{\partial z}\right)^2 + \left(\frac{\partial \bar{v}}{\partial z}\right)^2 \right] \right)^{1/2} \tag{4}$$

where l_h and l_v are horizontal and vertical mixing length scales respectively.

2.1.2. Boundary Conditions
In the numerical study here, the boundary conditions need to be set as [14]: by the bottom, by the surface of the water [17], by boundaries which can be vertical impermeable structures (wall), and by boundaries in the open sea [18]. The power available in the Manado Bay, we can be obtaining from Equation [19-20]:

$$P = \frac{1}{2}\rho(v)^3 10^{-3} \tag{5}$$

where P in kW/m2, v is $\sqrt{\bar{u}^2 + \bar{v}^2 + \bar{w}^2}$ (m/s) and ρ is density of water (kg/m³).

2.2. Numerical Model
The numerical method that used was semi-implicit finite difference for the 3D in Equation (1), (2), and (3) was used by: [1], [3], [12], [15], and [21-23].
Figure 1 shows choices adopt in the vertical direction. The velocities are defined on the edge of the mesh, we guessed virtual meshes to write the limiting conditions with the walls, and we decorate the free surface with the grid.
The generally, we can be written semi-implicit discretization in Equation (1) and (2) in the compact matrix form [1] as follow:

$$A_{i+1/2,j}^n U_{i+1/2,j}^{n+1} = G_{i+1/2,j}^n - g\frac{\Delta t}{\Delta x}\left(\eta_{i+1,j}^{n+1} - \eta_{i,j}^{n+1}\right)\Delta Z_{i+1/2,j}^n \tag{6}$$

$$A_{i,j+1/2}^n V_{i,j+1/2}^{n+1} = G_{i,j+1/2}^n - g\frac{\Delta t}{\Delta y}\left(\eta_{i,j+1}^{n+1} - \eta_{i,j}^{n+1}\right)\Delta Z_{i,j+1/2}^n \tag{7}$$

Then, the velocity vertical in Equation (3) becomes:

$$\overline{w}_{i,j,k+1/2}^{n+1} = \overline{w}_{i,j,k-1/2}^{n+1} - \frac{\Delta z_{i+1/2,j,k}^{n}\overline{u}_{i+1/2,j,k}^{n+1} - \Delta z_{i-1/2,j,k}^{n}\overline{u}_{i-1/2,j,k}^{n+1}}{\Delta x}$$

$$- \frac{\Delta z_{i,j+1/2,k}^{n}\overline{v}_{i,j+1/2,k}^{n+1} - \Delta z_{i,j-1/2,k}^{n}\overline{v}_{i,j-1/2,k}^{n+1}}{\Delta y}$$

(8)

If we are discretization Equation (5), then the power available becomes:

$$P = \frac{1}{2}\rho \ (v_{i,j,k}^{n+1})^{3}10^{-3}$$

(9)

where P is the availability power in the Manado Bay (kW/m^2) and $v_{i,j,k}^{n+1} = \sqrt{\overline{u}^2 + \overline{v}^2 + \overline{w}^2}$ is velocity resultant with $\overline{u} = \frac{1}{2}(\overline{u}_{i,j,k}^{n+1} + \overline{u}_{i+1,j,k}^{n+1})$, $\overline{v} = \frac{1}{2}(\overline{v}_{i,j,k}^{n+1} + \overline{v}_{i,j+1,k}^{n+1})$ and $\overline{w} = \frac{1}{2}(\overline{w}_{i,j,k}^{n+1} + \overline{w}_{i,j,k+1}^{n+1})$ are scalars, respectively.
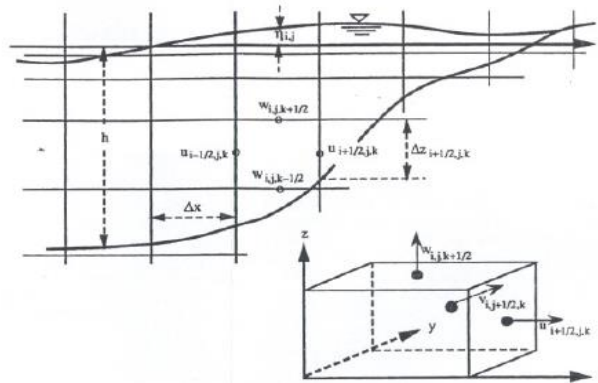

Figure 1. Meshes and notations for computational (2D and 3D)

3. Method

Figure 2 shows flow chart for solution of a numerical model in calculating the velocities of $\overline{u}$, $\overline{v}$ and $\overline{w}$ respectively and the power available in the Manado Bay. The "calculate components of the velocities (u, v and w) and power available" symbol are show a process for calculating of horizontal velocities $\overline{u}$ in Equation 6 and $\overline{v}$ in Equation 7 with a linear three-diagonal, whereas for calculating velocity vertical $\overline{w}$ use Equation (8). Finally, calculating the power available where the calculation used Equation (9). The "n" symbol shows the quantity of calculating with iteration do-process until maximum iteration (T_{max}). The "T > T_{max}" symbol is the process to execute determination when the iteration has been greater than maximum iteration, if no then process will be go to "n" for continue to calculate again, and if yes then it go to "finish".

The position of Manado Bay in Indonesia and numerical area are located in the Sulawesi Sea with approximately 300 km^2 of the area as shown in Figure 3 and width of about 2.2 km between Bunaken Island and Sulawesi Island, and down to 79 m deep.

We are made two types of simulations in 3D-simulations with one discharge. There are four layers to deep. In calculation, there are 174 x 318 mesh in x, y directions with $\Delta x = \Delta y =$ 7 m. Also, we are used four vertical layers and the integration time $\Delta t = 0.4$ sec as shown in Table 1, and discharge is 0.1 Sv (1 Sv = 10^6 m^3/s). Figure 4 illustrates the bathymetry 3-D and 2D of the Manado Bay which used for numerical simulation.

Tide predictions were computed based on the Admiralty method using Harmonic Constants taken from the Indonesia Sailing Direction and the results of the Hydro-Oceanographic surveys. Information about tide is needed for the safety of navigation as mention in navigational Indonesia regulation number 21, 1992 [24]. Hourly heights of tide of 95 stations

in Indonesia are given for whole period in one year. Time used in local standard time. Predictions refer to Chard Datum of Low Water Spring. Height should be added to charted depths, unless preceded by minus sign (-) then they should be subtracted. Water heights are given in Meter. It is pointed that though the prediction in the tide tables, in substance gives the actual movements of tide.

Table 1. Numerical parameter for 3D-simulations

Parameter	Value	Parameter	Value
G	9.81 m s^{-2}	P	1024 kg/m^3
C_z	48	Δx	7 m
τ_o	2 days	Δy	7 m
τ_i	1 day	Δz	1 m
Discharge	0.1 Sv	Δt	0.4 sec

START

READ DATA

GENERATION OF THE MESH (dz)

GENERATION OF THE INDEX (ivf)

INITIAL CONDITIONS

n

BOUNDARY CONDITIONS

CALCULATE ADVECTIONS IN U AND V

TURBULENCE VISCOSITY

CALCULATE FREE SURFACES

CALCULATE COMPONENTS OF THE VELOCITIES (U, V AND W) AND POWER AVAILABLE

PRINT RESULTS

no $T>T_{max}$

yes

STOP

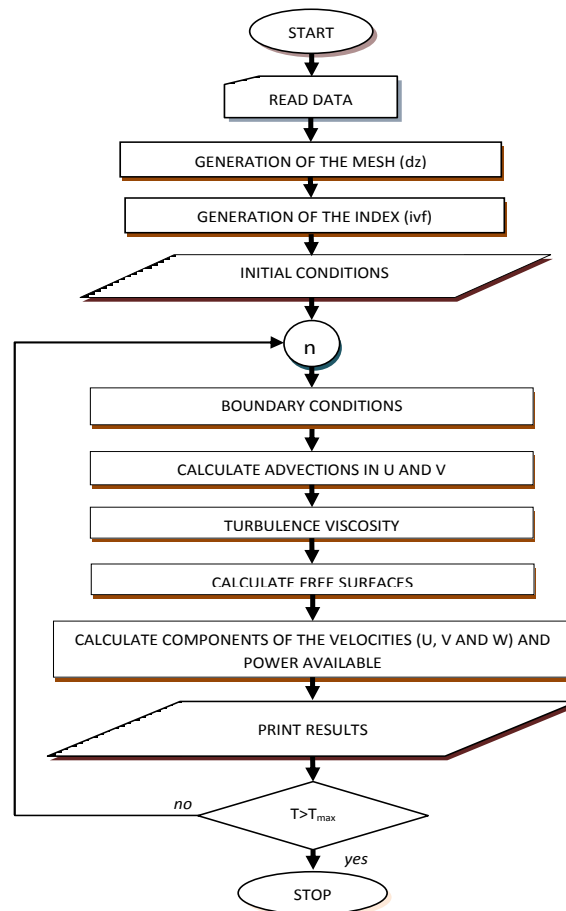Figure 2. Flow chart of a numerical model

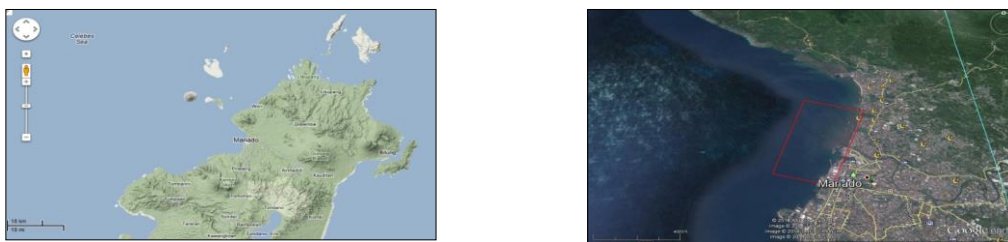Figure 3. The position of Manado Bay in Indonesia and numerical area

(a)   (b)
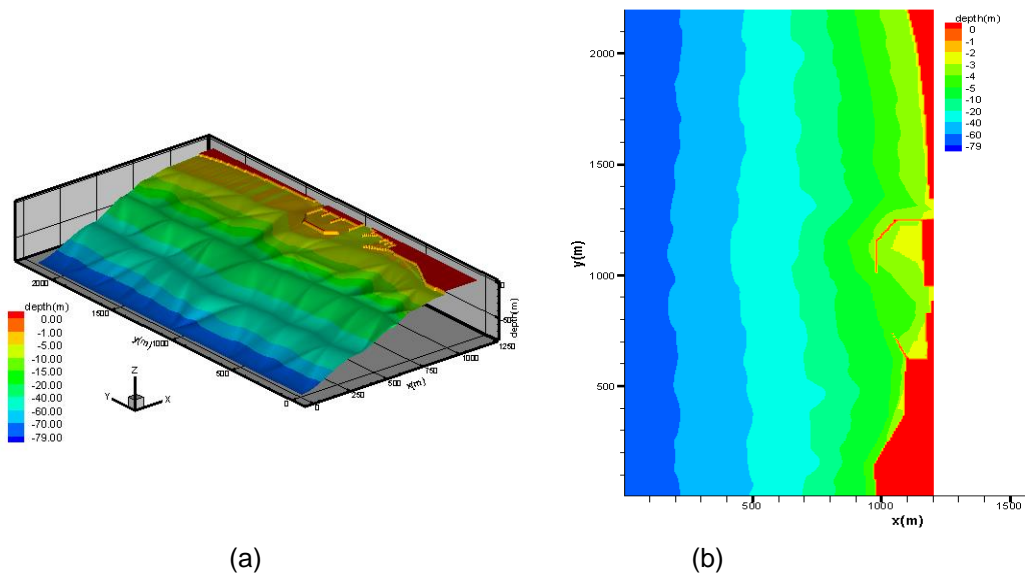
Figure 4. The bathymetry of the Manado Bay in 3D (a) and 2D (b)

4. Results and Discussion

We can see that the power available distributions when high tide currents (Figure 6b) at in front of the Singkil river downstream (Figure 4b) where around 80-105 kW/m^2 bigger than the other area in around that of 1-60 kW/m^2. It caused by existence of manger and average depth in the place of ~5 m. Also, in West area, especially at centre area where power availabilities around 16-20 kW/m^2. Whereas in North area where the power available still less unless in South area about 30-50 kW/m^2. Figure 5 shows the tide predictions for 37 days from on 16 January to 21 February 2014 [24]. Predictions refer to Chart Datum 1.2 m under Mean Sea Level (MSL). The type of tides is mixed, mainly semidiurnal and some of that are diurnal.

If we see in Westside (left hand) where there are power availabilities biggest around 10-15 kW/m^2. When low tide currents (Figure 6. a) at in front of the Singkil river, East-North, and East-South, where around 15-20 kW/m^2. Whereas at enter channel in Singkil river of 0.5-8 kW/m2. It is caused due to the confluence of the river and the marine currents, also, the flow of river water to move freely into the sea with an average depth of 2 m.
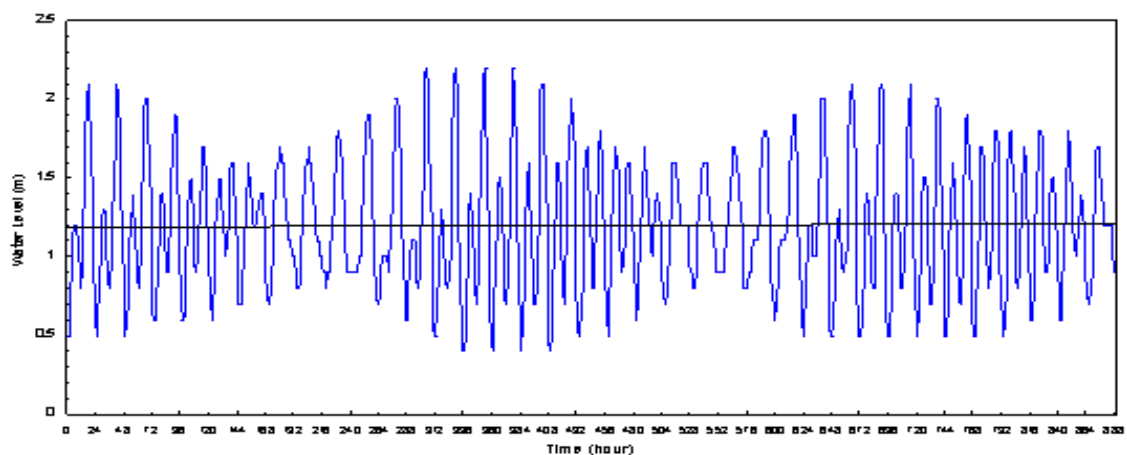

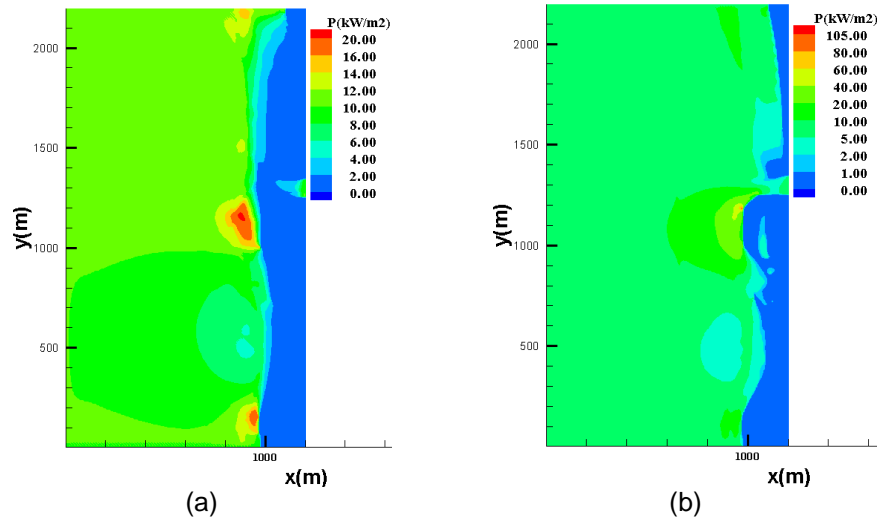Figure 5. Tide predictions of the Manado Bay

Figure 6. 2D-Simulated distributions of the power available when low tide currents (a) and high tide currents (b) in the Manado Bay
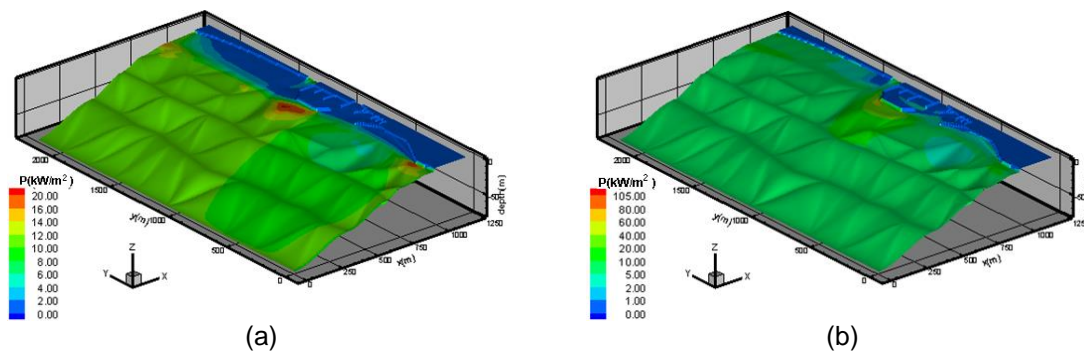

Figure 7. 3D-Simulated distributions of the power available when low tide currents (a) and high tide currents (b) in the Manado Bay

The distributions of the power available when low and high tide currents in the Manado Bay (3D-simulation) at discharge 0.1 Sv respectively showed in Figure 7. Tide currents very influence to the power available which very big at high tide current [25-27]. When low tide currents, the distributions were 0.00-20.00 kW/m^2 and 0.00-105.00 kW/m^2 when high tide currents in the Manado Bay.

4. Conclusion

Study on marine current in the Manado Bay, North Sulawesi, Indonesia through a numerical model has been successfully accomplished. The maximum of power available at discharge of 0.1 Sv when low and high tide currents were 20 and 105 kW/m^2 respectively. The results will be enabling to design the turbines that used in the marine current power plant in Manado Bay in the future.

Acknowledgements

References

[1]   Casulli V, Cheng RT. Semi-implicit finite difference methods for three-dimensional shallow water flow. *International Journal for Numerical Methods in Fluids*. 1992; 15: 629-648.

[2]   Clement JL, Maslowski W, Cooper LW, Grebmeier JM, Walczowski W. Ocean circulation and exchanges through the northern Bering Sea-1979-2001 model results. *Deep-Sea Research II*. 2005; 52: 3509-3540.

[3]   Zarrati AR, Jin YC. Development of a generalized multi-layer model for 3-D simulation of free surface flows. *International Journal for Numerical Methods in Fluids*. 2004; 46: 1049-1067.

[4]   Rompas PTD, Manongko JDI. Numerical simulation of marine currents in the Bunaken Strait, North Sulawesi, Indonesia. *IOP Conference Series: Materials Science and Engineering*. 2016; 128(012003): 1-7.

[5]   Draper S, Borthwick AGL, Houlsby GT. Energy potential of a tidal fence deployed near a coastal headland. *Philosophical Transaction of the Royal Society A*. 2013; 371: 1-16.

[6]   Chen J–L, Hsu T-J, Shi F. Raubenheimer, B. & Elgar, S. Hydrodynamic and sediment transport modeling of New River Inlet (NC) under the interaction of tides and waves. *Journal of Geophysical Research: Oceans*. 2015: 4028-4047.

[7]   Caliskan U, Fuhrman DR. RANS-based simulation of wave-induced sheet-flow transport of graded sediments. *Coastal Engineering*. 2017; 121: 90-102.

[8]   Zhang C, Zheng J-H, Zhang J-S. Predictability of wave-induced net sediment transport using the conventional 1DV RANS diffusion model. *Geo-Marine Letters*. 2014; 34: 353-364.

[9]   Tang L, Lin P. Numerical modeling of oscillatory turbulent boundary layer flows and sediment suspension. *Journal of Ocean Engineering and Marine Energy*. 2014: 1-12.

[10]   Walters RA. A coastal ocean model with subgrid approximation. *Ocean Modelling*. 2016; 102: 45-54.

[11]   Sedigh M, Tomlinson R, Cartwright N, Etemad-Shahidi A. Numerical modeling of the Gold Coast Seaway area hydrodynamics and littoral drift. *Ocean Engineering*. 2016; 121: 47-61.

[12]   Gu Y, Gong M, Li H. Application of Remote Sensing Axis Line Method in Xiaomiaohong Creek. *TELKOMNIKA Indonesian Journal of Electrical Engineering*. 2014; 12(5): 3323-3330.

[13]   Elzalabani MM, Fahmy FH, Nafeh AESA, Allam G. Modelling and Simulation of Tidal Current Turbine with Permanent Magnet Synchronous Generator. *TELKOMNIKA Indonesian Journal of Electrical Engineering*. 2015; 13(1): 57-64.

[14]   Hervouet JM. Hydrodynamics of free surface flows: Modelling with the finite element method. England: John Wiley & Sons Ltd. 2007: xiv-341.

[15]   Stansby PK. A mixing-length model for shallow turbulent wakes. *Journal of Fluid Mechanics*. 2003; 495: 369-384.

[16]   Cea L, French JR, Vazquez-Cendon ME. Numerical modelling of tidal flows in complex estuaries including turbulence: An unstructured finite volume solver and experimental validation. *International Journal for Numerical Methods in Engineering*. 2006; 67: 1909-1932.

[17]   Chen X. A free-surface correction method for simulating shallow water flows. *Journal of Computational Physics*. 2003; 189: 557-578.

[18]   Treguier AM, Barnier B, De Miranda AP. An eddy-permitting model of the Atlantic circulation: Evaluating open boundary condition. *Journal of Geophysical Research: Oceans*. 2001; 106: 1-23.

[19]   Hydro BC. Green energy study for British Columbia-phase 2-mainland tidal current energy. Triton Consultants Ltd.
       http://www.llbc.leg.bc.ca/public/PubDocs/bcdocs/357590/environment3928.pdf. (10 February 2012).

[20]   Luquet R, Bellevre D, Fréchou D, Perdon P, Guinard P. Design and model testing of an optimized ducted marine current turbine. *International Journal of Marine Energy*. 2013; 2: 61-80.

[21]   Stansby PK. Semi-implicit finite volume shallow-water flow and solute transport solver with k-Ɛ turbulence model. *International Journal for Numerical Methods in Fluids*. 1997; 25: 285-313.

[22]   Rodriguez C, Serre E, Rey C, Ramirez H. A numerical model for shallow-water flows: dynamics of the eddy shedding. *WSEAS Transactions on Environment and Development*. 2005; 1: 280-287.

[23]   Casulli V, Walters RA. An unstructured grid, three-dimensional model based on the shallow water equations. *International Journal for Numerical Methods in Fluids*. 2000; 32: 331-348.

[24]   Daftar pasang surut (tide tables). Kepulauan Indonesia (Indonesian Archipelago). Jakarta: Dinas Hidro-Oceanografi TNI AL. 2014.

[25]   Rompas PTD, Taunaumang H, Sangari FJ. A Numerical Design of Marine Current for Predicting Velocity and Kinetic Energy. *Indonesian Journal of Electrical Engineering and Computer Science*. 2017; 5(2): 401-409.

[26]   Rompas PTD, Taunaumang H, Sangari FJ. A Numerical Model of Seawater Volume and Velocity Dynamic for Marine Currents Power Plant in the Bangka Strait, North Sulawesi, Indonesia. *IOP Conference Series: Materials Science and Engineering*. 2017; 180(012100): 1-7.

[27]   Rompas PTD, Sangari FJ, Tanunaumang H. Study on Marine Current with Approach of a Numerical Model for Marine Current Power Plant (PLTAL) in the Bangka Strait North Sulawesi. *Proceedings-2016 International Seminar on Application of Technology for Information and Communication, ISEMANTIC 2016. IEEE*. 2017: 104-110.